Received: 2 April 2020 | Revised: 22 October 2020 | Accepted: 17 November 2020

DOI: 10.1111/geb.13238

Check for updates

RESEARCH PAPER

Global Ecology and Biogeography A Journal of Macroecology WILEY

Caught in a bottleneck: Habitat loss for woolly mammoths in central North America and the ice-free corridor during the last deglaciation

Yue Wang[1,2] | Chris Widga[3] | Russell W. Graham[4] | Jenny L. McGuire[1,5,6] | Warren Porter[7] | David Wårlind[8] | John W. Williams[2,9]

[1]School of Biological Sciences, Georgia Institute of Technology, Atlanta, Georgia, USA

[2]Department of Geography, University of Wisconsin-Madison, Madison, Wisconsin, USA

[3]Center of Excellence in Paleontology, East Tennessee State University, Johnson City, Tennessee, USA

[4]Department of Geology and Geological Engineering, Colorado School of Mines, Golden, Colorado, USA

[5]Interdisciplinary Graduate Program in Quantitative Biosciences, Georgia Institute of Technology, Atlanta, Georgia, USA

[6]School of Earth and Atmospheric Sciences, Georgia Institute of Technology, Atlanta, Georgia, USA

[7]Department of Integrative Biology Research, University of Wisconsin-Madison, Madison, Wisconsin, USA

[8]Department of Physical Geography and Ecosystem Sciences, Lund University, Lund, Sweden

[9]Center for Climatic Research, University of Wisconsin-Madison, Madison, Wisconsin, USA

Correspondence
Yue Wang, School of Biological Sciences, Georgia Institute of Technology, 310 Ferst Dr., Atlanta, GA 30332, USA.
Email: yue.wang.pku@gmail.com

Funding information
National Science Foundation, Grant/Award Number: ARC-1203772, DEB-1353896 and DEB-1655898

Editor: Kathleen Lyons

Abstract

Aim: Identifying how climate change, habitat loss, and corridors interact to influence species survival or extinction is critical to understanding macro-scale biodiversity dynamics under changing environments. In North America, the ice-free corridor was the only major pathway for northward migration by megafaunal species during the last deglaciation. However, the timing and interplay among the late Quaternary megafaunal extinctions, climate change, habitat structure, and the opening and reforestation of the ice-free corridor have been unclear.

Location: North America.

Time period: 15–10 ka.

Major taxa studied: Woolly mammoth (*Mammuthus primigenius*).

Methods: For central North America and the ice-free corridor between 15 and 10 ka, we used a series of models and continental-scale datasets to reconstruct habitat characteristics and assess habitat suitability. The models and datasets include biophysical and statistical niche models Niche Mapper and Maxent, downscaled climate simulations from CCSM3 SynTraCE, LPJ-GUESS simulations of net primary productivity (NPP) and woody cover, and woody cover based upon fossil pollen from Neotoma.

Results: The ice-free corridor may have been of limited suitability for traversal by mammoths and other grazers due to persistently low productivity by herbaceous plants and quick reforestation after opening 14 ka. Simultaneously, rapid reforestation and decreased forage productivity may have led to declining habitat suitability in central North America. This was possibly amplified by a positive feedback loop driven by reduced herbivory pressures, as mammoth population decline led to the further loss of open habitat.

Main conclusions: Declining habitat availability south of the Laurentide Ice Sheet and limited habitat availability in the ice-free corridor were contributing factors in North American extinctions of woolly mammoths and other large grazers that likely operated synergistically with anthropogenic pressures. The role of habitat loss and attenuated corridor suitability for the woolly mammoth extinction reinforce the critical

 © 2020 John Wiley & Sons Ltd

importance of protected habitat connectivity during changing climates, particularly for large vertebrates.

KEYWORDS

climate adaptation, habitat loss, ice-free corridor, late Quaternary extinctions, LPJ-GUESS, Maxent, migration bottleneck, Niche Mapper, woolly mammoth

1 | INTRODUCTION

Habitat loss and fragmentation are the leading drivers of species extinction, with climate change becoming an increasing risk (IPBES, 2019). The effects of habitat loss and fragmentation are particularly severe for large vertebrates, which require abundant food sources and large habitat areas to support viable populations (Crooks et al., 2017; Ripple et al., 2017). Movement corridors mitigate extinction risk by facilitating animal tracking of climate change via movements to other available habitats (Dalén et al., 2007; Heintzman et al., 2016; Raia et al., 2012). However, movement corridors must be suited to particular species, possessing a suitable habitat for dispersal and transient survival (Baguette et al., 2013; Bowler & Benton, 2005). Given that nearly one-quarter of species have a high risk of extinction (IPBES, 2019) and that the Earth system is approaching rates and magnitudes of climate change unseen since the end of the last glacial period, if ever (Burke et al., 2018; Williams et al., 2019), a key research need is to understand whether and how corridors can mitigate local habitat losses during rapid climate change, thereby facilitating species adaptation to climate change and maintaining biodiversity and ecosystem services.

During the late Quaternary, nearly two-thirds of terrestrial megafaunal genera went extinct worldwide (Barnosky et al., 2004), with size-selective extinctions beginning as early as 125 ka (F. A. Smith et al., 2018). Climatic and anthropogenic drivers likely co-contributed to the megafaunal extinctions (e.g. Barnosky et al., 2004; Surovell et al., 2016), with megafaunal species responding individualistically to the effects of climate change, habitat shifts, and growing human populations (Lorenzen et al., 2011). In temperate latitudes, regional habitat destabilization and rapid vegetation change during the last deglaciation may have contributed to the megafaunal extinctions in synergy with anthropogenic pressures (Blois & Hadly, 2009; Di Febbraro et al., 2017; Ficcarelli et al., 2003; Haynes, 2013; Mann et al., 2019; Nogués-Bravo et al., 2010; Wang et al., 2020; Wroe et al., 2013). A key knowledge frontier is to better understand the particular interactions of climate, habitat, human pressures, and regional geography for each extinction.

In North America, 35 megafaunal genera went extinct during the end of the last glacial period, with at least 16 genera dying out between 13.8 and 11.4 ka (thousands of years before present, defined as 1950 AD; Faith & Surovell, 2009). This period encompassed the expansion of human populations south of the Laurentide Ice Sheet, beginning *c*. 15 ka (Waters, 2019), and multiple large and abrupt climate changes (Buizert et al., 2014). In North America, the opening of the ice-free corridor between the Laurentide and Cordilleran Ice Sheets created both an immigration pathway for humans into the Americas and an escape pathway northwards for cold-adapted species as temperatures rose and regional climates became less favourable (Heintzman et al., 2016; Jass et al., 2011; Pedersen et al., 2016). The ice-free corridor may have opened as early as 14.9 ka (Waters, 2019), with evidence of megafaunal (bison) traversal northwards by 13.4 ka (Heintzman et al., 2016). However, for most megafaunal species in North America, the timing and interplay between megafaunal extinction, climate change, habitat availability, and the opening of the ice-free corridor remains unclear.

Here we assess the availability of the ice-free corridor as an escape pathway northward for woolly mammoths and other primarily grazer megafauna, by modelling both the declines in habitat availability south of the Laurentide Ice Sheet and habitat availability in the ice-free corridor itself, all during the critical window of rapidly changing climates and vegetation between 15 and 10 ka. We use two state-of-the-art approaches to independently evaluate the ecological suitability of habitats for woolly mammoths: a mechanistic biophysical niche model (Niche Mapper, Kearney & Porter, 2009) and a statistical species distribution model (Maxent, Hijmans et al., 2017). These models are driven by climatic and environmental characteristics, including downscaled climate simulations from the CCSM3 SynTraCE experiments (Lorenz et al., 2016), net primary productivity simulated by the dynamic vegetation model LPG-GUESS (Smith et al., 2001, 2014), and woody cover distributions based both upon fossil pollen networks from the Neotoma Paleoecology Database (Williams et al., 2011, 2018) and LPJ-GUESS (Figure 1).

We focus on woolly mammoths (*Mammuthus primigenius*) because they are one of the emblematic megafaunal species that went extinct during the end-Pleistocene extinctions and are representative of large nonruminant herbivores that mostly graze. We estimate their habitat availability in the Upper Midwest because of the rich fossil record in this region and well-documented collapse (Widga et al., 2017). Woolly mammoths were distributed in open steppe-like environments across the high latitudes of the Northern Hemisphere (Guthrie, 2006). They were primarily grazers, with a diet dominated by graminoids and herbs (Willerslev et al., 2014; Zimov et al., 2012), though some authors suggest a degree of mixed-feeding of graze and browse (Rivals et al., 2010; Saunders et al., 2010). Woolly mammoth populations on the North American mainland declined steeply starting at 14 ka and were extirpated by 12.1 ka (Guthrie, 2006; MacDonald et al., 2012; Widga et al., 2017). In these analyses, we seek to (a) evaluate the viability of the ice-free corridor as an escape route for megaherbivore grazer populations seeking to adapt to changing climates by shifting their ranges northward, and (b) assess

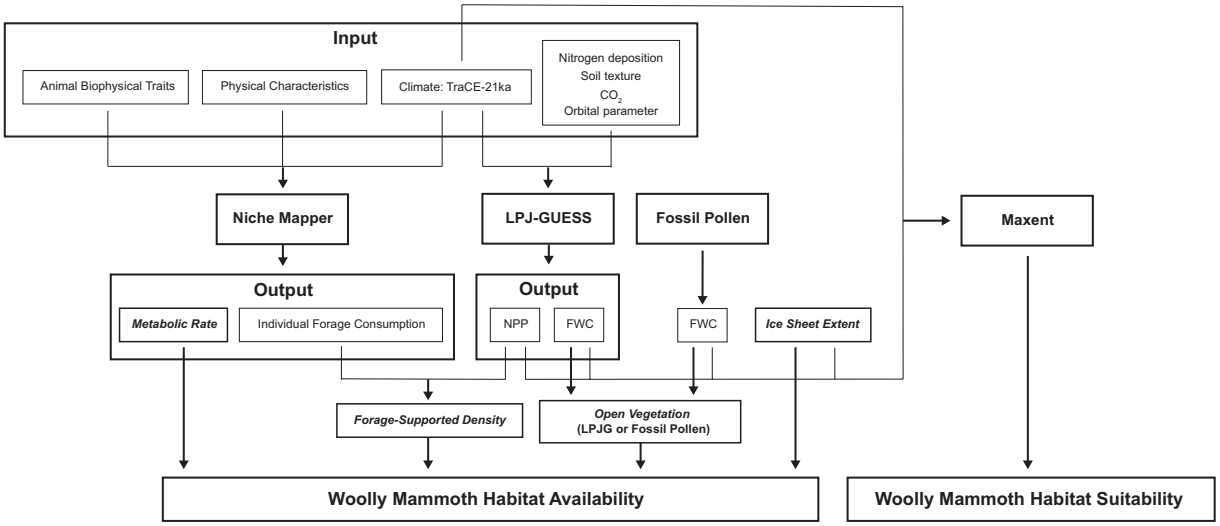


FIGURE 1 Experimental design, showing ecological models (Niche Mapper and Maxent), driver datasets, output variables, and derived predictions of habitat availability and suitability. Woolly mammoth habitat availability and suitability are predicted in parallel by Niche Mapper and Maxent. Inputs into these models include climate data, annual net primary productivity (NPP), and fractional woody cover (FWC). FWC is both reconstructed from fossil pollen data and simulated by LPJ-GUESS (LPJG). LPJ-GUESS uses climate, nitrogen deposition, soil texture, CO_2, and orbital insolation parameters to simulate both FWC and NPP for each plant functional type (PFT). Niche Mapper integrates animal biophysical traits, geological substrate, and climate (monthly minima and maxima of daily averages for temperature, relative humidity, cloud coverage, and wind speed) to simulate metabolic rate and forage consumption for individual woolly mammoths. Niche Mapper, in combination with NPP (from LPJG) and FWC (both LPJG- and pollen-derived), outputs three factors used to identify regions with suitable habitats for woolly mammoth: (a) metabolic rate > basal metabolic rate of woolly mammoth, (b) forage-supported density > minimum viable population (MVP) of woolly mammoth, in which forage-supported density is calculated from forage NPPs and individual woolly mammoth forage consumption, (c) open vegetation (defined as open grasslands and open forests). Maxent simulates habitat suitability based on climate data [annual mean temperature, annual mean precipitation, annual maximum temperature, annual minimum temperature, growing degree days (0 °C), growing degree days (5 °C), and water deficit calculated as potential evaporation minus actual evaporation], forage NPP, and FWC (both LPJG- and pollen-derived)

the timing of declines in woolly mammoth populations and habitat suitability in the midcontinental US relative to the timing of the ice-free corridor opening and its infilling by post-glacial afforestation.

2 | METHODS

2.1 | Study design: Overview

Our study design predicts changes in habitat availability and suitability for woolly mammoth populations in the ice-free corridor and central North America, using independent biophysical and statistical models (Niche Mapper and Maxent). Maxent calculates habitat suitability for mammoths, whereas Niche Mapper predicts habitat availability by energetic requirements for mammoths (see Figure 1 for model drivers, parameterization, and experimental design). These two models are driven by climate simulations and estimates of vegetation net primary productivity (NPP) and fractional woody cover (FWC). Climate simulations are from the downscaled CCSM3 SynTraCE experiment in North America (Lorenz et al., 2016). The NPP of vegetation was simulated by LPJ-GUESS (LPJG; Figure 2c). FWC was both simulated by LPJ-GUESS (Figure 2a) and independently reconstructed from fossil pollen and modern-analogue methods calibrated to remotely sensed observations (Williams et al., 2011) (Figure 2b). In the Niche Mapper simulations, these inputs were used to simulate metabolic rates and forage consumption rates and estimate habitat availability (Figure 2d–f). In the Maxent simulations, nine climate variables, forage NPP, and FWC are predictors for habitat suitability (Figure 2g,h). We trained Maxent using fossil woolly mammoth records from previously published compilations for North America (Enk et al., 2016; MacDonald et al., 2012; Widga et al., 2017) and the Neotoma Paleoecology Database (http://www.neotomadb.org, Williams et al., 2018). All input datasets and simulations used a spatial resolution of 0.5° × 0.5° grid latitude and longitude. These analyses were conducted at a temporal resolution of 100-year means of climate simulations every 1,000 years, from 15 to 10 ka. Simulations were run for all of North America except Alaska (10°–80° N, 140°–45° W), because of possible inaccuracies in the CCSM3 SynTraCE temperature simulations for Alaska (Otto-Bliesner et al., 2006; Wang et al., 2018), with focused analyses for the ice-free corridor and Upper Midwest (Figures 2–4).

2.2 | Palaeoclimate: CCSM3 SynTraCE

Climate inputs were drawn or calculated from the CCSM3 SynTraCE simulations of deglacial climates (He et al., 2013; Z. Liu et al., 2009), downscaled from a native resolution of *c.* 3.75° × *c.* 3.75° to 0.5° ×

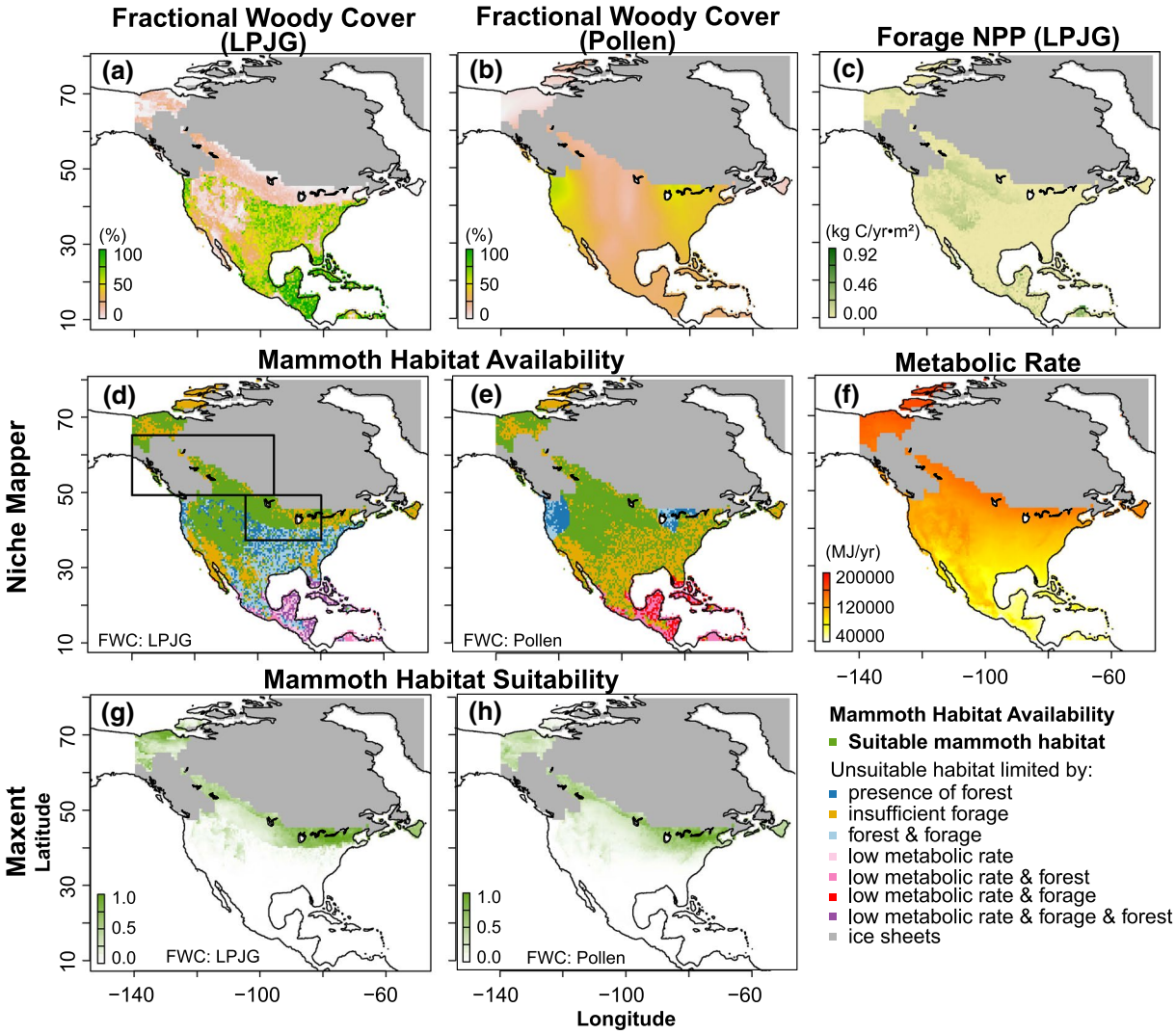


FIGURE 2 Simulated habitat availability and suitability for mammoths by Niche Mapper and Maxent at 13 ka and underlying predictor variables, including inputs (a) LPJ-GUESS-simulated fractional woody cover (FWC), (b) pollen-reconstructed FWC (Williams et al., 2011), (c) net primary productivity (NPP) of forage-available plant functional types simulated by LPJ-GUESS. Subsequent panels show model results: (d) simulated suitable habitat by Niche Mapper based on LPJ-GUESS-simulated FWC and (e) pollen-reconstructed FWC, (f) Niche-Mapper simulated metabolic rate, (g,h) habitat suitability by Maxent based on LPJ-GUESS-simulated FWC and pollen-reconstructed FWC, respectively. Boxes in (d) show inset maps for Upper Midwest (Figures 3 and 5) and ice-free corridor (Figures 4 and 5). Ice sheet extent is from ICE-6G (Peltier et al., 2015). Green colour in (d) and (e) (the colour of the top panel in the legend of habitat availability) indicates available habitat by Niche Mapper. See Figure 1 for explanations of habitat limits represented by other colours in (d) and (e)

0.5° (Lorenz et al., 2016). All monthly data in the SynTraCE output used here represent decadal-scale averages, which we then averaged to centennial-scale averages to represent typical environments for each of the 1-ka intervals in the Niche Mapper, Maxent, and LPJ-GUESS simulations. Monthly temperature minima/maxima/average values and monthly precipitation average values are directly from the Lorenz et al. (2016) downscaled CCSM3 SynTraCE simulation. For other climate variables, including monthly minima/maxima/average values of cloud coverage, wind speed, relative humidity, we either downscaled the monthly values from SynTraCE decadal seasonal averages using the methods described in Lorenz et al. (2016) or calculated the inputs from other climate variables (see Supporting Information Appendix S1).

2.3 | Palaeovegetation: LPJ-GUESS and fossil pollen data

Forage NPP was simulated using LPJ-GUESS, while FWC was generated independently from LPJ-GUESS simulations and fossil pollen reconstructions. LPJ-GUESS is a dynamic vegetation and terrestrial ecosystem model that predicts vegetation structure, composition, and productivity, given information about climate variables, atmospheric CO_2, nitrogen deposition, solar degrees, and soil characteristics (B. Smith et al., 2001, 2014). We simulated NPP and FWC for 20 plant functional types (PFTs) in North America (Supporting Information Table S1.1). Monthly temperature, precipitation, and monthly cloud coverage were the same

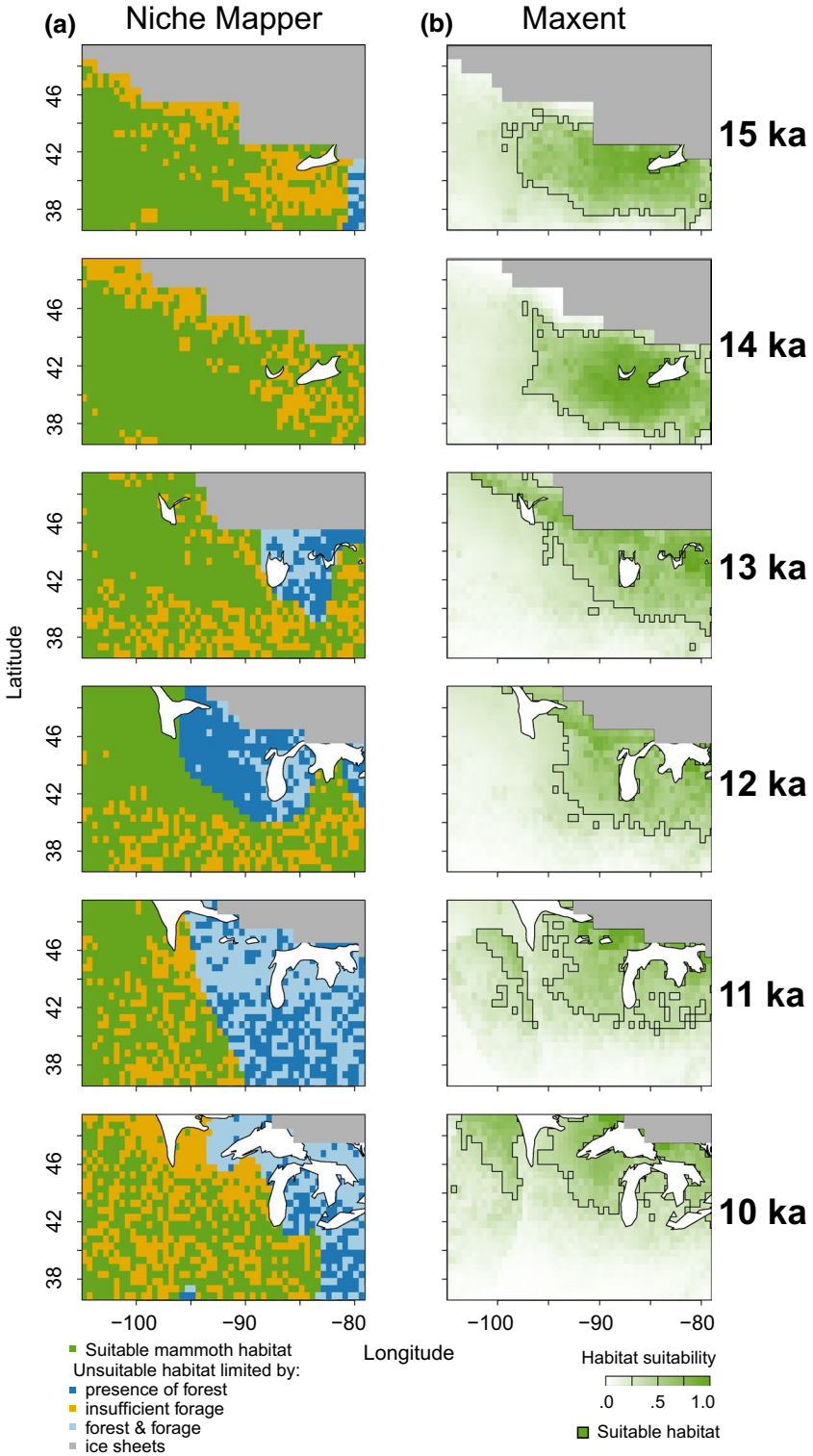


FIGURE 3 Maps of available habitat simulated by Niche Mapper (a) and habitat suitability simulated by Maxent (b) for mammoths in the Upper Midwest. In (b), the grid cells of binary suitable habitat are outlined by black lines. Fractional woody cover (FWC) inputs for these models are based on fossil pollen records; see Supporting Information Figure S2.14 for versions based on LPJ-GUESS (LPGJ)-derived FWC for the Upper Midwest. Both models show declining habitat suitability over time, while differing in intraregional patterns

as for Niche Mapper (Lorenz et al., 2016). Atmospheric CO_2 concentrations were from the EPICA ice core, averaged at the centennial scale for each 1,000-year snapshot (Monnin et al., 2004; Supporting Information Table S1.2). Monthly nitrogen deposition was set to constant pre-industrial 1850 AD values from the ACCMIP database (Lamarque et al., 2013). We calculated incoming solar radiation using a modified form of the equations built into LPJ-GUESS to account for orbitally driven changes in insolation (Berger, 1978; Crucifix, 2016; Supporting Information Table S1.3). For further details, see Supporting Information Appendix S1.

For FWC, we also used an independent set of reconstructions from 770 fossil pollen sites (Williams et al., 2011). The site-level FWC was estimated using the modern analogue technique, in which modern pollen samples were cross-referenced to remotely sensed

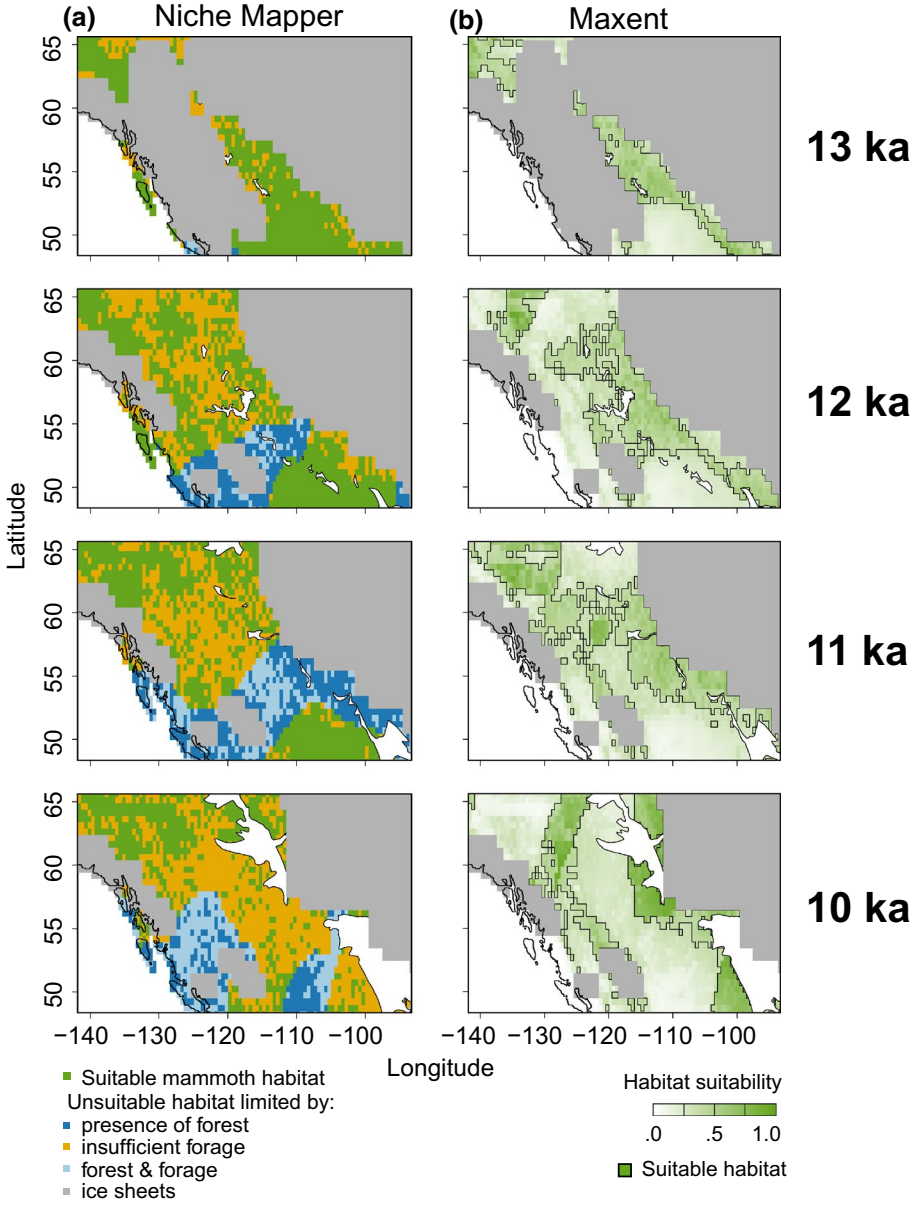


FIGURE 4 Maps of available habitat area for mammoths in the ice-free corridor simulated by Niche Mapper (a) and the suitability of habitat occurrence simulated by Maxent (b). As with Figure 3, the distribution of fractional woody cover (FWC) is based on pollen, and grid cells of binary suitable habitat are outlined by black lines in (b). See Supporting Information Figure S2.15 for habitat suitability based on LPJ-GUESS (LPJG)-derived FWC. Both models indicate widespread areas of low habitat suitability or availability in the ice-free corridor

observations of contemporary FWC. The resulting reconstructions of past forest cover were at a temporal resolution of every 500 years, from 21 ka to present (Williams et al., 2011). We spatially interpolated the site-level fractional woody cover to a resolution of 0.5° × 0.5° by kriging (Cressie, 1990).

For Niche Mapper and Maxent, we estimated the available habitat based on both the pollen-reconstructed and LPJ-GUESS-simulated estimates of FWC (Figure 1). Simulations based on the pollen reconstructions of FWC are reported in the main text and those based on the LPJ-GUESS simulations of FWC are reported in Supporting Information Appendix S2.

2.4 | Niche Mapper

Niche Mapper is a mechanistic niche model that simulates the energetic balances for individual animals in equilibrium with their ambient environment (Kearney & Porter, 2009). Niche Mapper receives inputs of biophysical traits (Supporting Information Table S1.4) and environmental variables (Supporting Information Table S1.5, Figure S1.1) and uses these to simulate local hourly microclimates that constrain the heat and mass balances for individual animals in steady state with their local environment. We developed estimates of biophysical traits for woolly mammoth in previous work

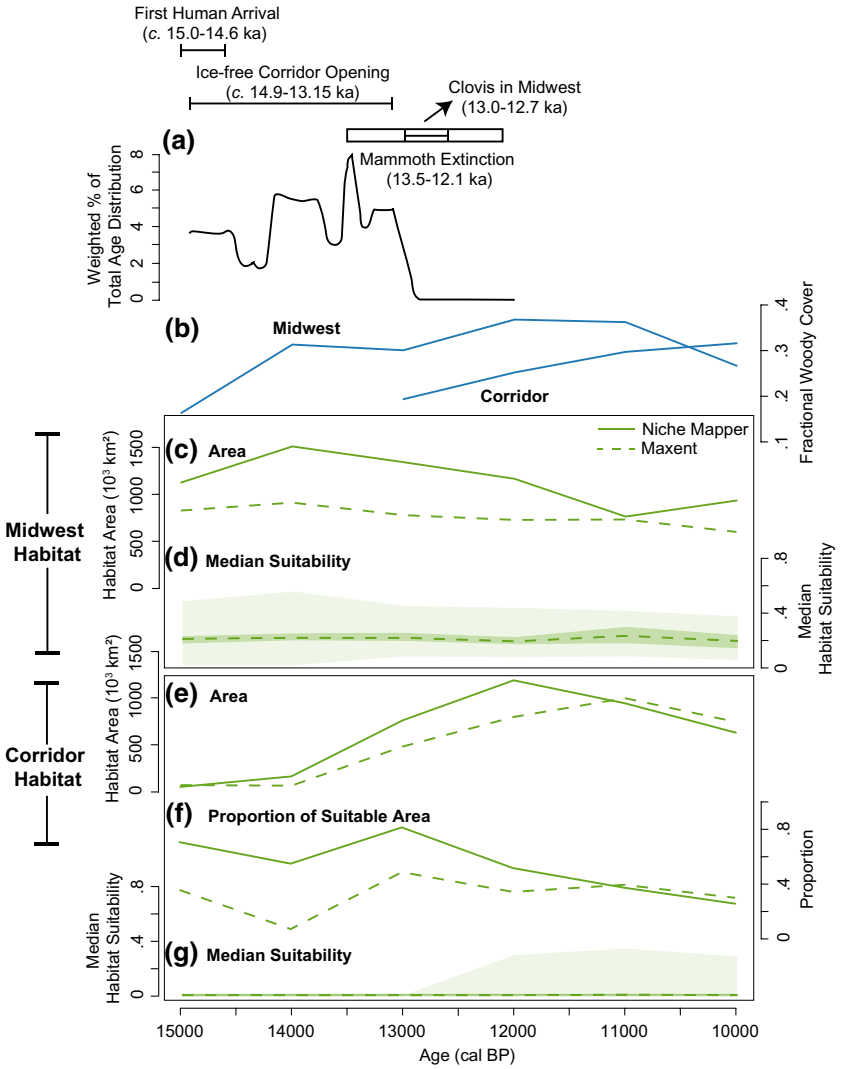


FIGURE 5 Time series of woolly mammoth extinction (Widga et al., 2017), human arrival (Waters, 2019) and corridor opening (a); mean fractional woody cover in the Midwest and the ice-free corridor based on fossil pollen data (b); available habitat area (Niche Mapper and Maxent) and habitat suitability (Maxent) for mammoths in the Upper Midwest (c,d) and the ice-free corridor (e–g). Solid curves represent results from Niche Mapper; dashed curves represent Maxent. For (d,g), the dark shading indicates the interquartile range among Maxent ensemble members with respect to their regional median suitability, while the light shading indicates the interquartile range of suitability among individual grid cells. During the extinction window for woolly mammoth in the Upper Midwest, based on radiocarbon dating of mammoth fossils (a) (Widga et al., 2017), habitat availability in the Upper Midwest was flat or declining, while availability in the ice-free corridor was low but rising

(Wang et al., 2018), including fur length, fur depth, core temperature, basal metabolic rate and dietary composition (Supporting Information Table S1.4). Climate inputs to Niche Mapper include (a) monthly minima and maxima of daily averages in temperature, wind speed, cloud coverage and relative humidity, and (b) monthly means of snow presence/absence, surface albedo, maximum shade percentage, and percent of unit area acting as a free water surface. For further details on the input datasets used for Niche Mapper, see Supporting Information Appendix S1.

For the Niche Mapper simulations, we predicted available habitat (Figure 2d,e) based on four criteria. First, the metabolic rate of the average individual woolly mammoth (Figure 2f) must be higher than the basal metabolic rate (Supporting Information Table S1.4), which represents a hard limit for survival (Mathewson et al., 2017; Supporting Information Appendix S1). Second, the NPP of forage PFTs (Figure 2c) must support a minimum viable mammoth population of 100 individuals (Sukumar, 1993) given Niche-Mapper-calculated forage consumption rates (Supporting Information Appendix S1) and an available forage area approximated at 4,000 km^2 (Hoppe et al., 1999), which is consistent with home range sizes for African elephants (Ngene et al., 2017). Third, the FWC must be low enough to support grazer populations and enable the movement of large mammoths (Figure 2a,b), with a threshold of 45% based on the maximum tree cover of open land (FAO, 1998) and the pollen-based estimated FWC related to the woolly mammoth fossil occurrences (Supporting Information Appendix S1). Finally, a grid cell must be ice-free, based on ice reconstructions from ICE-6G (VM5a) (Argus et al., 2014; Peltier et al., 2015) downscaled to 0.5° × 0.5° latitude/longitude. After predicting available habitat, we calculated the area of available habitat for each 1-ka interval from 15 to 10 ka.

2.5 | Maxent

We used the Maxent species distribution model (*dismo* in R 4.0.2., 2020; Hijmans et al., 2017; Phillips et al., 2020) to estimate habitat suitability for mammoths from 15 to 10 ka. For Maxent inputs, we used nine downscaled climate variables [annual minima/maxima/average temperature and precipitation, annual average growing degree days (base 0 °C), growing degree days (base 5 °C), and water deficit (calculated as potential evaporation minus actual evaporation)] and two habitat and resource variables

(FWC and forage NPP). Though the input variables are correlated, Maxent is robust to the collinearity of input variables by downplaying the role of redundant variables through model complexity regularization (Feng et al., 2019).

To train Maxent, we compiled 25 fossil woolly mammoth occurrences from between 20 and 12 ka (Supporting Information Table S1.6, Figure S1.2) from previously published compilations of directly dated specimens (Enk et al., 2016; MacDonald et al., 2012; Widga et al., 2017) and the FAUNMAP holdings in the Neotoma Paleoecology Database (Williams et al., 2018). Recent mitochondrial DNA (mtDNA) analyses illustrate the relationship between location and *Mammuthus* phylogenetics (Enk et al., 2016). We included localities that either exhibited morphological characteristics of woolly mammoths or were located within the region represented by Enk et al.'s (2016) Clade I (haplogroups D, E and C). We only included fossil woolly mammoth occurrences when age error uncertainty (one sigma error range) is fewer than 500 years and when the climate uncertainty within age error uncertainty is smaller than 3 °C and 300 mm (Supporting Information Figure S1.3, see also Appendix S1). We then converted all radiocarbon ages to calendar ages using IntCal20 (Reimer et al., 2020). For the background points, we collected 10,000 background points from 20 to 12 ka in North America except Alaska and regions covered by ice or lakes (Supporting Information Table S1.7; Barbet-Massin et al., 2012). Randomly selecting background points from across a too-broad climate-space can exacerbate spatial biases, compromising model accuracy (Kramer-Schadt et al., 2013). To minimize this issue and ensure accurate Maxent calibration, we followed a stratified random sampling design for background points that matches the spatio-temporal distribution of fossil occurrences. In this stratified design, we ensured proportional temporal sampling by setting a constant 400:1 ratio of background points to occurrences for a total of 10,000 background points. Then for each 1-ka interval, we employed a stratified spatial sampling design in which we randomly selected 50% of points from within a fossil buffer region and 50% points outside the fossil buffer region, in which the buffer radius is set at 25 km based on the 99% nearest neighbourhood distances between fossil localities (see details in Supporting Information Appendix S1). This buffer background sampling method can reduce the errors of over-prediction caused by a too-broad climate-space of widespread mammoth occurrences (Barbet-Massin et al., 2012).

We ran Maxent 100 times with different background points to predict the suitability of woolly mammoth habitat in North America from 15 to 10 ka at a spatial resolution of 0.5° × 0.5° grid. Each time we randomly selected 75% of the occurrence and background data as training data and the other 25% as validation data. We calculated the area under the curve (AUC) value of the validation data to select the best-fit models. We projected the Maxent models with AUC values higher than .80 onto each 1-ka interval from 15 to 10 ka (Phillips & Dudík, 2008). Then we calculated the median and mean values of habitat suitability in the Midwest and ice-free corridor for each 1-ka interval. For each interval, we also calculated the area of available habitat, for which the threshold for suitable habitat was set as the value that maximizes the sum of sensitivity and specificity (SSS) in the fitted models (C. Liu et al., 2013).

2.6 | Statistical tests

We performed two types of statistical analyses to explore whether the habitat availability in the Upper Midwest and ice-free corridor changed significantly between 14 and 11 ka. This period encompasses the woolly mammoth extinction window of 13.5 to 12.1 ka (Widga et al., 2017). For the area of available habitat by Niche Mapper and Maxent, we fitted the area by linear regression and calculated the *p*-value of the linear regression model. The low *p*-value (< .05) suggests that available habitat changed significantly in this period. For the suitability of habitat from Maxent, in order to incorporate spatial heterogeneity, we performed a *t* test on habitat suitability at every grid cell per 1-ka interval from the 100 repeats of Maxent simulations. Then we counted grid cells where the predicted habitat suitability changed significantly.

3 | RESULTS

3.1 | Niche Mapper model results

Simulated metabolic rates were higher in the high latitudes than in the low latitudes and were higher at 15 than 10 ka (Supporting Information Figure S2.4). These relationships occur because mammoths and other endotherms thermoregulate in part by maintaining a higher metabolic rate in colder environments, to offset higher rates of heat loss to the ambient environment. As a result, southern North America was not suitable for woolly mammoths due to the lower-than-basal metabolic rates under the hot climate in the tropics (Supporting Information Figures S2.10 and S2.11). Simulated forage consumption rates were also higher in high latitudes and colder time periods than in the low latitudes and warmer time periods (Supporting Information Figure S2.5), resulting from the higher rates of energy consumption needed to support a higher metabolic rate. However, despite the lower forage consumption rates in higher latitudes and colder time periods, the simulated forage-supported mammoth population densities were lower for these times and regions (Supporting Information Figure S2.6), because of the even larger decreases in forage NPP (Supporting Information Figure S2.7) due to both low-temperature downregulation of NPP and rapid postglacial reforestation (Supporting Information Figures S2.8 and S2.9). In the Upper Midwest and ice-free corridor, habitats remained energetically suitable for woolly mammoth (Figures 3a and 4a). However, forage-supported density significantly declined by a factor of 10 in these regions, from 254 individuals per 10^3 km^2 at 15 ka to 16 individuals per 10^3 km^2 at 10 ka in the Midwest (*p*-value < .05) and 305 individuals per 10^3 km^2 at 12 ka to 23 individuals per 10^3 km^2 at 10 ka in the ice-free corridor (*p*-value = .09).

3.2 | Maxent model validation and fitting

The fitted Maxent models perform well in predicting mammoth habitat suitability (Supporting Information Table S2.8, Figures S2.12 and S2.13). The AUC values for both the training and validation data are > .8, suggesting that the fitted models can distinguish the fossil occurrences from the background points (Phillips & Dudík, 2008). The omission rate is lower than .1 for the tenth percentile training presence threshold, indicating that the models are not overfitted (Radosavljevic & Anderson, 2014). The optimal sum of sensitivity and specificity (SSS) threshold is determined to be .37 (Supporting Information Table S2.8). At this threshold, the maximum omission rate is .026, meaning that Maxent has a 2.6% chance of reporting a false absence at a known occurrence of woolly mammoth.

3.3 | Changes in habitat availability in the Upper Midwest and ice-free corridor

In the Upper Midwest, habitat availability for woolly mammoths declined between 14 and 11 ka, with the largest decline simulated by Niche Mapper, primarily due to post-glacial reforestation (Figures 3 and 5c, Supporting Information Figures S2.10, S2.11, S2.14 and S2.16). The declines are strongest for simulations using pollen-based estimates of FWC. Using pollen-based FWC, the available habitat simulated by Niche Mapper decreased by nearly 50% from $1{,}510 \times 10^3$ km^2 at 14 ka to 763×10^3 km^2 at 11 ka (Figures 3a and 5c, green colour; p-value = .03 in the linear model), and the largest decline happened between 12 and 11 ka from $1{,}166 \times 10^3$ to 763×10^3 km^2. Suitable habitat area as calculated using Maxent also declined, but by a smaller proportion (21%), from 889×10^3 km^2 at 14 ka to 704×10^3 km^2 at 11 ka (Figures 3b and 5c, grid cells outlined by black line), and the decrease was not statistically significant across the entire Midwest (p-value = .11). However, within the Midwest, habitat suitability decreased significantly for 44 to 58% of grid cells between 14 and 11 ka, with the largest net loss between 14 and 13 ka (58% grid cells decreased suitability, 31% increases) and between 11 and 10 ka (58% grid cells decreased suitability, 17% increased) (Table 1). Forest expansion in the south and east Midwest contributed to nearly 25% of the habitat suitability decline (Table 2). This post-glacial forest expansion may have reduced woolly mammoth habitat by hampering mammoth movements and the decreased forage productivity. Some of the afforestation after 12 ka and declined in habitat suitability may represent increased woody coverage following reduced megaherbivory.

TABLE 1 Proportions of grid cells in the Upper Midwest where the predicted habitat suitability changed significantly, in which the predicted probabilities are from Maxent based on pollen-based fractional woody cover (FWC)

Time	Habitat suitability decrease	Habitat suitability increase
15–14 ka	.26	.45
14–13 ka	.58	.31
13–12 ka	.44	.27
12–11 ka	.46	.38
11–10 ka	.58	.17

At the same time, habitat availability in the ice-free corridor was limited by low grassland productivity and rapid tree expansion, suggesting that the corridor may have acted as a potential filter for mammoth habitat and migration (Figures 4 and 5e–g, Supporting Information Figures S2.10, S2.11, S2.15 and S2.17). Total area in the ice-free corridor increased as ice retreated, including area identified as potentially suitable habitat (Figure 5e). However, the proportion of area identified as suitable habitat generally declined (Figure 5f) and median habitat suitability was near-zero for all time periods (Figure 5g). The low suitability of the ice-free corridor was primarily due to the rapid expansion of tree taxa and persistently low abundances of forage PFTs (Figure 4). Across the ice-free corridor, low forage productivity was a major limit to habitat availability, with a good agreement between areas identified as forage-limited by Niche Mapper (Figure 4a, yellow) and low habitat suitability by Maxent (Figure 4b). LPJ-GUESS simulations indicate very low grassland productivities in the corridor (Supporting Information Figure S2.7), resulting in low maximum population densities of mammoths (Supporting Information Figure S2.6). Rapid tree expansion into the corridor is supported by both pollen records and LPJ-GUESS (Figure 5b, Supporting Information Figures S2.8 and S2.9).

Niche Mapper and Maxent do not predict exactly the same interregional patterns of suitable woolly mammoth habitats, but both models predict a habitat suitability decline in the Midwest and persistently low suitability in the ice-free corridor (Figure 5c–g). Both models support the role of forest expansion in the habitat suitability decline. Intraregional differences between models in predicted patterns of habitat availability (Figures 3 and 4) can be traced to differential weightings of individual environmental factors. Annual

TABLE 2 Maxent metrics for input variable contribution proportions. Input variables include annual mean/min/max temperature (AMT/AMinT/AMaxT), annual mean/min/max precipitation (AMP/AMinP/AMaxP), growing degree days (0 °C) (GDD0), growing degree days (5 °C) (GDD5), climate water deficit (CWD), fractional woody cover (FWC), and forage net primary productivity (NPP). For FWC, we used the simulations from LPJ-GUESS (LPJG) and fossil pollen, separately

	AMT	AMinT	AMaxT	AMP	AMinP	AMaxP	GDD0	GDD5	CWD	FWC	NPP
FWC-pollen	.06	.24	< .01	.05	.02	.04	.01	.24	.13	.25	.01
FWC-LPJG	.07	.32	< .01	.07	.10	.05	.02	.24	.10	.05	.01

minimum temperature and growing degree days (5 °C) contribute more than 45% to the habitat suitability in Maxent (Table 2), while in Niche Mapper climate does not directly affect habitat availability (Supporting Information Figure S2.14). These intermodel differences are most apparent in the Midwest (Figure 3), where Niche Mapper predictions of availability are strongly governed by forest expansion, while Maxent predictions are jointly governed by rising temperatures and changing vegetation.

4 | DISCUSSION

4.1 | Contributing factors to extinction: Climate change, corridors, and anthropogenic pressures

Disentangling the relative contributions of human populations and environmental changes to the late Quaternary extinctions has remained an active and sometimes contentious topic for decades (Barnosky et al., 2004; Mann et al., 2019; Surovell et al., 2016). The relative importance of anthropogenic and climatic drivers of extinction varied widely among megafaunal taxa (Lorenzen et al., 2011). The analyses here have focused on geographic and environmental factors that may have contributed to the extinctions of woolly mammoths and other large cold-adapted grazers and mixed feeders during the crucial extinction window of 14 to 11 ka, yet the ultimate extinction of many megafaunal species was presumably caused by a synergy between anthropogenic and environmental factors. Here we have elucidated in detail how in North America, the limited habitat suitability of the ice-free corridor may have contributed to the extinction of woolly mammoths during the crucial extinction window of 14 to 11 ka, while leaving open the question of to what degree anthropogenic pressures also contributed.

Range shifts are a primary mechanism by which species adapt to climate change, past and present (Lawler et al., 2013; McGuire et al., 2016; Ordonez & Williams, 2013; Pecl et al., 2017; Raia et al., 2012). The ice-free corridor that opened up between the Laurentide and Cordilleran Ice Sheets would have been the first available corridor for megafaunal populations south of the Laurentide Ice Sheet to move northwards as temperatures rose (Heintzman et al., 2016; Jass et al., 2011; Pedersen et al., 2016). These simulations, however, strongly suggest that the ice-free corridor may have been of only limited suitability for mammoths and open as an escape pathway for a short period of time. The corridor could have opened no earlier than 14.9 ka and the earliest evidence of cross-corridor animal migration (by bison) dates to 13.15 ka (Heintzman et al., 2016; Waters, 2019; Figure 5a). The persistently low forage productivity and rapid post-glacial reforestation of the ice-free corridor by spruce and other boreal tree taxa (Figure 5b; Ritchie & MacDonald, 1986; Williams et al., 2004) may have limited the northward dispersal of megafaunal grazers.

Concurrently, in eastern North America, rates of habitat reorganization were high (Wang et al., 2020), and open conifer and mixed conifer–hardwood parklands were lost, replaced by a Holocene arrangement of grasslands and eastern mesic forests (Williams et al., 2004). These losses of Pleistocene open parklands may have reduced the habitat availability for megafaunal species (Blois & Hadly, 2009; Di Febbraro et al., 2017; Ficcarelli et al., 2003; Graham, 1986; Haynes, 2013), increased competition among megafauna species, and thus increased the extinction risk of the woolly mammoth. Mammoths shared habitats characterized by herb-steppe-tundra vegetation with other megafaunal species, such as mastodon, caribou and muskox (e.g. Burns, 1996; Widga et al., 2017). During the last deglaciation (15–10 ka), much of the herb-steppe-tundra habitat across North America was lost, often replaced by wetland and forest (Barnosky et al., 2004; Strong & Hills, 2005; Willerslev et al., 2014). The competition among the megafauna species may have increased due to the loss of habitat, with survival pressure potentially exacerbated by overlapping dietary niches among species (Schwartz-Narbonne et al., 2019). Isotopic analyses suggest that, in response to changing environments, large herbivores had a high level of dietary flexibility and were capable of utilizing both C_3 and C_4 plants (Feranec, 2004; Widga et al., 2020), bison were able to shift their dietary niche to low $\delta^{15}N$ food sources and caribou had an adaptable diet with varying consumptions of browsing and lichen, while mammoth had a consistently high $\delta^{15}N$ value in the diet (Rabanus-Wallace et al., 2017; Schwartz-Narbonne et al., 2019). Our modelling results suggest that the expansion of post-glacial forest and the low productivity of the herbaceous vegetation in the corridor may have supported only limited populations and increased resource competition among megafaunal species with dietary overlaps, thereby enhancing the extinction risk of woolly mammoth.

The decline and extinction of woolly mammoth populations also may have reinforced Midwestern landscape changes. Open habitat ideally suited to woolly mammoths declined after 14 ka, with much of the decline occurring between 12 and 10 ka, after the extinction window (Figures 3 and 5b,c, Table 1). This suggests that the loss of woolly mammoth may have exacerbated the loss of landscape openness, perhaps by the selective release of palatable plant taxa from herbivore pressure (Gill, 2014). Large herbivores can maintain vegetation openness by high biomass consumption and woody regeneration suppression (C. N. Johnson, 2009). Multi-proxy studies of fossil pollen, coprophilous spores, and sedimentary charcoal from lake sediments suggest that the loss of keystone herbivores altered the plant community structure and ecosystem function by the release of hardwoods from herbivore pressure and the spread of fire regimes through accumulated fuels (Gill et al., 2009, 2012; Rule et al., 2012), although other studies have reported weaker signals of megafauna on vegetation composition (Jeffers et al., 2018). In our work, the Niche Mapper and LPG-GUESS models used here do not include the effects of megafaunal herbivory on vegetation biomass and composition and so these simulations do not incorporate possible megafaunal vegetation effects. However, pollen-based estimates of woody cover in the Midwest increased sharply between 13 and 12 ka, immediately after the decline in woolly mammoth (Figure 5a,b), and remained high after the population went extinct. This observed afforestation is partially attributable to rising temperatures

(Fastovich et al., 2020) but may also indicate that woolly mammoths, as ecosystem engineers, played important roles in landscape transformation. These landscape transitions may also have acted as a positive feedback loop of habitat loss (Wang et al., 2020) that exacerbated the woolly mammoth population decline and extinction. A next step forward is to include megaherbivory in mechanistic dynamic vegetation models such as LPJ-GUESS; such models are at the early stages of development (Pachzelt et al., 2013, 2015).

Our analyses suggest decreases in available habitat area in the Midwest rather than complete loss, suggesting that environmental pressures alone were not enough to drive Midwestern populations to extinction. Overall, these modelling results suggest that habitat suitability was declining in the Upper Midwest (Figure 5c,d), although the patterns and trends are not as clear as in the ice-free corridor (Figure 5e–g). Instead, these analyses are consistent with hypotheses proposing that megafaunal extinctions were driven by a synergy between anthropogenic pressures and changing climates and habitats. Southern mammoth populations, partially trapped by a bottlenecked corridor, would have been vulnerable to increased rates of mortality due to intensified predation by humans, as human population sizes grew and new technologies and toolkits were developed. Increased human pressure is proposed as the main driver for megafaunal extinction globally (e.g. Lyons et al., 2004; F. A. Smith et al., 2018). The strong body size selectivity of the late Quaternary extinctions is anomalous prior to early Cenozoic mammalian extinctions, and can be explained by either selective hunting by humans or non-selective harvesting extinction combined with higher vulnerability of large-bodied animals due to their life history characteristics (Zuo et al., 2013).

The archaeological record in North America remains incomplete and open to multiple interpretations. Moreover, at a continental scale, the chronological overlap between human presence and megafaunal extinctions is indicative of anthropogenic contributions to late Pleistocene extinctions (Martin, 1984; Surovell et al., 2016), and consistent with a model in which several thousand years of increased human pressures and coexistence led to extinction, rather than abrupt blitzkrieg. However, direct zooarchaeological evidence of human hunting in the Upper Midwest and other key regions is fragmentary (E. Johnson, 2006) and has been disputed (Broughton & Weitzel, 2018; Grayson & Meltzer, 2015; Widga et al., 2017). The North American archaeological record of Clovis-era human/megafaunal associations is limited to only 15 well-substantiated instances across the continent (Grayson & Meltzer, 2015; Surovell et al., 2005); among these, only two that date to the time of extinction are located in the Midwest (Kimmswick, Pleasant Lake) and one near the southern terminus of the ice-free corridor (Wally's Beach). In all three cases, the subjects of human interaction were non-mammoth taxa (i.e. horse, camel, mastodon). Indeed, all dated archaeological sites are rare in the study area during the extinction window (12.5–13 ka) and site density in the Upper Midwest is one of the lowest in North America at the time (Chaput et al., 2015). The duration of megafaunal–human coexistence varied spatially in North America (Emery-Wetherell et al., 2017), as did the severity of human impacts. Hence, woolly mammoth populations south of the ice sheet were likely subjected to a synergistic combination of intensified human pressures, warming climates and at least regionally declining habitat suitability, but the exact contributions of these factors remain difficult to establish precisely.

This work does, however, highlight the critical role played by corridors in allowing large vertebrates to adapt to climate change. Such species usually are highly mobile and require large habitat areas, so high habitat connectivity helps these species to track and adjust to rapid climate change (McGuire et al., 2016). The projected rates and magnitudes of future global temperature rise are similar to or greater than those of the last deglaciation (Burke et al., 2018; Williams et al., 2019). The brief opening and limited suitability of the ice-free corridor during the extinction window of 14–11 ka offers an object lesson in how low connectivity can enhance extinction risk during periods of changing environments and intensified human pressures. Hence, these analyses support conservation policies that focus on maximizing habitat connectivity and minimizing the effects of synergistic drivers of species extinction. Contemporary pathway modelling is enabling increasingly detailed mappings of likely migration pathways for vertebrate species as climates change (Lawler et al., 2013). Such corridors connecting these pathways should be prioritized for conservation to protect biodiversity and may be particularly important for populations of large mobile herbivores.

4.2 | Niche Mapper and Maxent: Advantages and uncertainties

A key advance of this study is the use of two fundamentally different approaches to modelling the suitability of late Pleistocene and early Holocene habitats for woolly mammoth. Niche Mapper and Maxent agree well with respect to broad patterns (a habitat suitability decline in the Midwest and a migration bottleneck in the ice-free corridor) while differing in the intraregional patterns of habitat availability. As a first-principles bioenergetics model, Niche Mapper should be robust to challenges faced by correlative distributional models when extrapolated into past and future climates with no modern analogue (Mathewson et al., 2017). Niche Mapper simulations are sensitive, however, to parameterization of animal traits, which for mammoths are based on direct measurement of their bones and soft tissue remains, a literature review, and estimates from their closest extant analogues, African elephants (Wang et al., 2018). The simulated forage consumption rate is particularly sensitive to hair density, digestive efficiency and body mass (Wang et al., 2018). Denser hairs, higher digestive efficiency and smaller body mass lead to lower forage consumption rate and higher potential population densities. Previous work suggests that the maximum possible woolly mammoth population density could be three times as high as estimated here, given upper-end estimates of 4,170 hairs/cm^2, which is the hair density of musk ox (Flood et al., 1989), 3,900 kg adult body mass, which is the lower-end estimate from fossil bones, and +15% digestive efficiency (Wang et al., 2018). However, even in this optimal scenario,

forage limits to population density would still intensify in the Upper Midwest after 11 ka as tree populations expanded (99 individuals per 10^3 km^2), and the ice-free corridor would still have difficulty supporting a minimum viable population.

Maxent, in contrast, is an empirical model that is based entirely on a statistical model of the realized niche for woolly mammoth, using the fossil occurrence data and palaeoclimatic simulations. The realized niche as simulated by Maxent is unlikely to be affected by dispersal limitation, given the potentially high mobility of mammoths and other elephantoid species (Widga et al., 2020). However, the fossil record is fragmentary and may be affected by non-climatic factors such as species interaction, human activities and fossil reservation. These fragmentary fossil records add uncertainty to the predicted available habitat by Maxtent. As a result, the niche reconstructed from mammoth fossil occurrences by Maxent is expected to be smaller than the fundamental niche of mammoth, which may lead to incompletely described species–climate relationships and underestimates of habitat suitability (Araujo & Guisan, 2006; Guisan & Thuiller, 2005; Kearney & Porter, 2009; Newbold, 2010).

Although each modelling framework has its limitations and uncertainties, as described above, the good similarity in findings between the two approaches strengthens the support for the conclusions reached here. Both models indicate declining habitat availability in the Midwest and both indicate that ice-free corridor would have had generally low habitat suitability during the critical window between 15 and 12.5 ka. Potential causes of intermodal differences in Midwestern habitat availability include uncertainties in environmental driver datasets, trait parameterization in Niche Mapper, and the relative weighting of environmental variables. Next steps to pursue include (a) more accurate measurements and fuller representation of biophysical traits in the mechanistic model, (b) incorporating woolly mammoth fossil occurrences in Eurasia in Maxent to better estimate the available habitat and extinction risk of woolly mammoth, and (c) expanding these approaches to other taxa.

5 | CONCLUSIONS

These analyses suggest that between 14 and 11 ka, mammoth populations south of the Laurentide Ice Sheet may have been increasingly challenged by declining habitat suitability, rising temperatures, reforestation, and reduced forage quality. These megafaunal populations presumably also were pressured by intensified competition with other megafaunal species and were more vulnerable to increased mortality rates due to growing human populations, although these processes were not directly studied here. Critically, the ice-free corridor itself, as the first available escape route northwards, appears to have been only of marginal suitability for mammoths, and open for perhaps only a thousand years or less around 13 ka, before being largely closed again by post-glacial reforestation. Habitat suitability in the ice-free corridor for mammoths was low due to rapid post-glacial tree expansion, low grassland productivity, and, overall, low forage supply. The limited availability of suitable habitat in the ice-free corridor would have exposed traversing megafaunal populations in the corridor to the synergistic effects of limited habitat availability and human hunting. The decline and extinction of woolly mammoths, as an important ecosystem engineer, may have amplified rates of afforestation and loss of open habitat, reinforcing extinction risk as a positive feedback loop. This study highlights the importance of corridors for species to adapt to changing climates and suggests that the ice-free corridor may have been less suitable for traversing megafaunal herbivores than previously realized. Because species are now adapting to climate changes via range shifts, increasing habitat connectivity among projected migration pathways is an essential conservation priority.

ACKNOWLEDGMENTS

We thank the Center for High Throughput Computing at the University of Wisconsin-Madison for providing computing services. We thank Ben Shipley for his suggestions on this work. This work was supported by the National Science Foundation awards ARC-1203772, DEB-1353896 and DEB-1655898.

DATA AVAILABILITY STATEMENT

All the data on palaeovegetation and woolly mammoth Niche Mapper results are available on Dryad: https://doi.org/10.5061/dryad.kkwh70s3k.

ORCID

Yue Wang https://orcid.org/0000-0002-9826-3276
Chris Widga https://orcid.org/0000-0002-2961-0078
Russell W. Graham https://orcid.org/0000-0002-4381-7788
Jenny L. McGuire https://orcid.org/0000-0002-0663-6902
Warren Porter https://orcid.org/0000-0003-0156-4222
David Wårlind https://orcid.org/0000-0002-6257-0338
John W. Williams https://orcid.org/0000-0001-6046-9634

REFERENCES

Araujo, M. B., & Guisan, A. (2006). Five (or so) challenges for species distribution modelling. *Journal of Biogeography*, *33*(10), 1677–1688. https://doi.org/10.1111/j.1365-2699.2006.01584.x

Argus, D. F., Peltier, W., Drummond, R., & Moore, A. W. (2014). The Antarctica component of postglacial rebound model ICE-6G_C (VM5a) based on GPS positioning, exposure age dating of ice thicknesses, and relative sea level histories. *Geophysical Journal International*, *198*(1), 537–563. https://doi.org/10.1093/gji/ggu140

Baguette, M., Blanchet, S., Legrand, D., Stevens, V. M., & Turlure, C. (2013). Individual dispersal, landscape connectivity and ecological networks. *Biological Reviews*, *88*(2), 310–326. https://doi.org/10.1111/brv.12000

Barbet-Massin, M., Jiguet, F., Albert, C. H., & Thuiller, W. (2012). Selecting pseudo-absences for species distribution models: How, where and how many? *Methods in Ecology and Evolution*, *3*(2), 327–338. https://doi.org/10.1111/j.2041-210X.2011.00172.x

Barnosky, A. D., Koch, P. L., Feranec, R. S., Wing, S. L., & Shabel, A. B. (2004). Assessing the causes of late Pleistocene extinctions on the continents. *Science*, *306*(5693), 70–75.

Berger, A. (1978). Long-term variations of daily insolation and Quaternary climatic changes. *Journal of the Atmospheric Sciences*, *35*(12), 2362–2367.

Blois, J. L., & Hadly, E. A. (2009). Mammalian response to Cenozoic climatic change. *Annual Review of Earth and Planetary Sciences*, *37*, 181–208. https://doi.org/10.1146/annurev.earth.031208.100055

Bowler, D. E., & Benton, T. G. (2005). Causes and consequences of animal dispersal strategies: Relating individual behaviour to spatial dynamics. *Biological Reviews*, *80*(2), 205–225. https://doi.org/10.1017/S1464793104006645

Broughton, J. M., & Weitzel, E. M. (2018). Population reconstructions for humans and megafauna suggest mixed causes for North American Pleistocene extinctions. *Nature Communications*, *9*(1), 1–12. https://doi.org/10.1038/s41467-018-07897-1

Buizert, C., Gkinis, V., Severinghaus, J. P., He, F., Lecavalier, B. S., Kindler, P., Leuenberger, M., Carlson, A. E., Vinther, B., & Masson-Delmotte, V. (2014). Greenland temperature response to climate forcing during the last deglaciation. *Science*, *345*(6201), 1177–1180.

Burke, K., Williams, J., Chandler, M., Haywood, A., Lunt, D., & Otto-Bliesner, B. (2018). Pliocene and Eocene provide best analogs for near-future climates. *Proceedings of the National Academy of Sciences USA*, *115*(52), 13288–13293. https://doi.org/10.1073/pnas.1809600115

Burns, J. A. (1996). Vertebrate paleontology and the alleged ice-free corridor: The meat of the matter. *Quaternary International*, *32*, 107–112. https://doi.org/10.1016/1040-6182(95)00057-7

Chaput, M. A., Kriesche, B., Betts, M., Martindale, A., Kulik, R., Schmidt, V., & Gajewski, K. (2015). Spatiotemporal distribution of Holocene populations in North America. *Proceedings of the National Academy of Sciences USA*, *112*(39), 12127–12132. https://doi.org/10.1073/pnas.1505657112

Cressie, N. (1990). The origins of kriging. *Mathematical Geology*, *22*(3), 239–252. https://doi.org/10.1007/BF00889887

Crooks, K. R., Burdett, C. L., Theobald, D. M., King, S. R., Di Marco, M., Rondinini, C., & Boitani, L. (2017). Quantification of habitat fragmentation reveals extinction risk in terrestrial mammals. *Proceedings of the National Academy of Sciences USA*, *114*(29), 7635–7640. https://doi.org/10.1073/pnas.1705769114

Crucifix, M. (2016). *palinsol: Insolation for palaeoclimate studies* (version R 0.93). Retrieved from https://bitbucket.org/mcrucifix/insol

Dalen, L., Nystrom, V., Valdiosera, C., Germonpre, M., Sablin, M., Turner, E., Angerbjorn, A., Arsuaga, J. L., & Gotherstrom, A. (2007). Ancient DNA reveals lack of postglacial habitat tracking in the arctic fox. *Proceedings of the National Academy of Sciences USA*, *104*(16), 6726–6729. https://doi.org/10.1073/pnas.0701341104

Di Febbraro, M., Carotenuto, F., Castiglione, S., Russo, D., Loy, A., Maiorano, L., & Raia, P. (2017). Does the jack of all trades fare best? Survival and niche width in Late Pleistocene megafauna. *Journal of Biogeography*, *44*(12), 2828–2838. https://doi.org/10.1111/jbi.13078

Emery-Wetherell, M. M., McHorse, B. K., & Davis, E. B. (2017). Spatially explicit analysis sheds new light on the Pleistocene megafaunal extinction in North America. *Paleobiology*, *43*(4), 642–655. https://doi.org/10.1017/pab.2017.15

Enk, J., Devault, A., Widga, C., Saunders, J., Szpak, P., Southon, J., Rouillard, J.-M., Shapiro, B., Golding, G. B., Zazula, G., Froese, D., Fisher, D. C., MacPhee, R. D. E., & Poinar, H. (2016). Mammuthus population dynamics in Late Pleistocene North America: Divergence, phylogeography, and introgression. *Frontiers in Ecology and Evolution*, *4*, 42. https://doi.org/10.3389/fevo.2016.00042

Faith, J. T., & Surovell, T. A. (2009). Synchronous extinction of North America's Pleistocene mammals. *Proceedings of the National Academy of Sciences USA*, *106*(49), 20641–20645. https://doi.org/10.1073/pnas.0908153106

FAO (1998). *The State of Food and Agriculture 1998* (No. 31). Rome, Italy: Food & Agriculture Org. Retrieved from http://www.fao.org/3/w9500e/w9500e.pdf.

Fastovich, D., Russell, J. M., Jackson, S. T., & Williams, J. W. (2020). Deglacial temperature controls on no-analog community establishment in the Great Lakes Region. *Quaternary Science Reviews*, *234*, 106245. https://doi.org/10.1016/j.quascirev.2020.106245

Feng, X., Park, D. S., Liang, Y., Pandey, R., & Papeş, M. (2019). Collinearity in ecological niche modeling: Confusions and challenges. *Ecology and Evolution*, *9*(18), 10365–10376. https://doi.org/10.1002/ece3.5555

Feranec, R. S. (2004). Geographic variation in the diet of hypsodont herbivores from the Rancholabrean of Florida. *Palaeogeography, Palaeoclimatology, Palaeoecology*, *207*(3–4), 359–369. https://doi.org/10.1016/j.palaeo.2003.09.031

Ficcarelli, G., Coltorti, M., Moreno-Espinosa, M., Pieruccini, P., Rook, L., & Torre, D. (2003). A model for the Holocene extinction of the mammal megafauna in Ecuador. *Journal of South American Earth Sciences*, *15*(8), 835–845. https://doi.org/10.1016/S0895-9811(02)00145-1

Flood, P. F., Stalker, M. J., & Rowell, J. E. (1989). The hair follicle density and seasonal shedding cycle of the muskox (*Ovibos moschatus*). *Canadian Journal of Zoology*, *67*(5), 1143–1147.

Gill, J. L. (2014). Ecological impacts of the late Quaternary megaherbivore extinctions. *New Phytologist*, *201*(4), 1163–1169. https://doi.org/10.1111/nph.12576

Gill, J. L., Williams, J. W., Jackson, S. T., Donnelly, J. P., & Schellinger, G. C. (2012). Climatic and megaherbivory controls on late-glacial vegetation dynamics: A new, high-resolution, multi-proxy record from Silver Lake, Ohio. *Quaternary Science Reviews*, *34*, 66–80. https://doi.org/10.1016/j.quascirev.2011.12.008

Gill, J. L., Williams, J. W., Jackson, S. T., Lininger, K. B., & Robinson, G. S. (2009). Pleistocene megafaunal collapse, novel plant communities, and enhanced fire regimes in North America. *Science*, *326*(5956), 1100–1103.

Graham, R. W. (1986). Response of mammalian communities to environmental changes during the late Quaternary. In J. Diamond & T. J. Case (Eds.), *Community Ecology* (pp. 300–313). New York: Harper and Row.

Grayson, D. K., & Meltzer, D. J. (2015). Revisiting Paleoindian exploitation of extinct North American mammals. *Journal of Archaeological Science*, *56*, 177–193. https://doi.org/10.1016/j.jas.2015.02.009

Guisan, A., & Thuiller, W. (2005). Predicting species distribution: Offering more than simple habitat models. *Ecology Letters*, *8*(9), 993–1009. https://doi.org/10.1111/j.1461-0248.2005.00792.x

Guthrie, R. D. (2006). New carbon dates link climatic change with human colonization and Pleistocene extinctions. *Nature*, *441*(7090), 207–209. https://doi.org/10.1038/nature04604

Haynes, G. (2013). Extinctions in North America's late glacial landscapes. *Quaternary International*, *285*, 89–98. https://doi.org/10.1016/j.quaint.2010.07.026

He, F., Shakun, J. D., Clark, P. U., Carlson, A. E., Liu, Z., Otto-Bliesner, B. L., & Kutzbach, J. E. (2013). Northern Hemisphere forcing of Southern Hemisphere climate during the last deglaciation. *Nature*, *494*(7435), 81. https://doi.org/10.1038/nature11822

Heintzman, P. D., Froese, D., Ives, J. W., Soares, A. E. R., Zazula, G. D., Letts, B., Andrews, T. D., Driver, J. C., Hall, E., Hare, P. G., Jass, C. N., MacKay, G., Southon, J. R., Stiller, M., Woywitka, R., Suchard, M. A., & Shapiro, B. (2016). Bison phylogeography constrains dispersal and viability of the Ice Free Corridor in western Canada. *Proceedings of the National Academy of Sciences USA*, *113*(29), 8057–8063. https://doi.org/10.1073/pnas.1601077113

Hijmans, R. J., Phillips, S., Leathwick, J., & Elith, J. (2017). *dismo: Species distribution modeling* (version 1.1-4). R package version (1 p.). Retrieved from http://rspatial.org/sdm/

Hoppe, K. A., Koch, P. L., Carlson, R. W., & Webb, S. D. (1999). Tracking mammoths and mastodons: Reconstruction of migratory behavior using strontium isotope ratios. *Geology*, *27*(5), 439–442.

IPBES (2019). *Summary for policymakers of the global assessment report on biodiversity and ecosystem services of the Intergovernmental Science-Policy Platform on Biodiversity and Ecosystem Services*. IPBES Secretariat.

Jass, C. N., Burns, J. A., & Milot, P. J. (2011). Description of fossil muskoxen and relative abundance of Pleistocene megafauna in central Alberta. *Canadian Journal of Earth Sciences*, *48*(5), 793–800. https://doi.org/10.1139/e10-096

Jeffers, E. S., Whitehouse, N. J., Lister, A., Plunkett, G., Barratt, P., Smyth, E., Lamb, P., Dee, M. W., Brooks, S. J., Willis, K. J., Froyd, C. A., Watson, J. E., & Bonsall, M. B. (2018). Plant controls on Late Quaternary whole ecosystem structure and function. *Ecology Letters*, *21*(6), 814–825. https://doi.org/10.1111/ele.12944

Johnson, C. N. (2009). Ecological consequences of Late Quaternary extinctions of megafauna. *Proceedings of the Royal Society B: Biological Sciences*, *276*(1667), 2509–2519.

Johnson, E. (2006). The taphonomy of mammoth localities in southeastern Wisconsin (USA). *Quaternary International*, *142*, 58–78. https://doi.org/10.1016/j.quaint.2005.03.005

Kearney, M., & Porter, W. (2009). Mechanistic niche modelling: Combining physiological and spatial data to predict species' ranges. *Ecology Letters*, *12*(4), 334–350. https://doi.org/10.1111/j.1461-0248.2008.01277.x

Kramer-Schadt, S., Niedballa, J., Pilgrim, J. D., Schröder, B., Lindenborn, J., Reinfelder, V., Stillfried, M., Heckmann, I., Scharf, A. K., Augeri, D. M., Cheyne, S. M., Hearn, A. J., Ross, J., Macdonald, D. W., Mathai, J., Eaton, J., Marshall, A. J., Semiadi, G., Rustam, R., … Wilting, A. (2013). The importance of correcting for sampling bias in MaxEnt species distribution models. *Diversity and Distributions*, *19*(11), 1366–1379. https://doi.org/10.1111/ddi.12096

Lamarque, J.-F., Dentener, F., McConnell, J., Ro, C., Shaw, M., Vet, R., & Doherty, R. (2013). Multi-model mean nitrogen and sulfur deposition from the atmospheric chemistry and climate model intercomparison project (ACCMIP): Evaluation of historical and projected future. *Atmospheric Chemistry and Physics*, *13*(16), 7997–8018.

Lawler, J., Ruesch, A., Olden, J., & McRae, B. (2013). Projected climate-driven faunal movement routes. *Ecology Letters*, *16*(8), 1014–1022. https://doi.org/10.1111/ele.12132

Liu, C., White, M., & Newell, G. (2013). Selecting thresholds for the prediction of species occurrence with presence-only data. *Journal of Biogeography*, *40*(4), 778–789. https://doi.org/10.1111/jbi.12058

Liu, Z., Otto-Bliesner, B., He, F., Brady, E., Tomas, R., Clark, P., Carlson, A.E., Lynch-Stieglitz, J., Curry, W., & Brook, E. (2009). Transient simulation of last deglaciation with a new mechanism for Bølling-Allerød warming. *Science*, *325*(5938), 310–314.

Lorenz, D. J., Nieto-Lugilde, D., Blois, J. L., Fitzpatrick, M. C., & Williams, J. W. (2016). Downscaled and debiased climate simulations for North America from 21,000 years ago to 2100AD. *Scientific Data*, *3*, 160048. https://doi.org/10.1038/sdata.2016.48

Lorenzen, E. D., Nogués-Bravo, D., Orlando, L., Weinstock, J., Binladen, J., Marske, K. A., Ugan, A., Borregaard, M. K., Gilbert, M. T. P., Nielsen, R., Ho, S. Y. W., Goebel, T., Graf, K. E., Byers, D., Stenderup, J. T., Rasmussen, M., Campos, P. F., Leonard, J. A., Koepfli, K.-P., … Willerslev, E. (2011). Species-specific responses of Late Quaternary megafauna to climate and humans. *Nature*, *479*(7373), 359–364. https://doi.org/10.1038/nature10574

Lyons, S. K., Smith, F. A., & Brown, J. H. (2004). Of mice, mastodons and men: Human-mediated extinctions on four continents. *Evolutionary Ecology Research*, *6*(3), 339–358.

MacDonald, G. M., Beilman, D. W., Kuzmin, Y. V., Orlova, L. A., Kremenetski, K. V., Shapiro, B., Wayne, R. K., & Van Valkenburgh, B. (2012). Pattern of extinction of the woolly mammoth in Beringia. *Nature Communications*, *3*(1), 1–8. https://doi.org/10.1038/ncomms1881

Mann, D. H., Groves, P., Gaglioti, B. V., & Shapiro, B. A. (2019). Climate-driven ecological stability as a globally shared cause of Late Quaternary megafaunal extinctions: The Plaids and Stripes Hypothesis. *Biological Reviews*, *94*(1), 328–352. https://doi.org/10.1111/brv.12456

Martin, P. S. (1984). Prehistoric overkill: The global model. P. Martin & R. Klein (Eds.), In *Quaternary extinctions: A prehistoric revolution* (pp. 354–403).

Mathewson, P. D., Moyer-Horner, L., Beever, E. A., Briscoe, N. J., Kearney, M., Yahn, J. M., & Porter, W. P. (2017). Mechanistic variables can enhance predictive models of endotherm distributions: The American pika under current, past, and future climates. *Global Change Biology*, *23*(3), 1048–1064. https://doi.org/10.1111/gcb.13454

McGuire, J. L., Lawler, J. J., McRae, B. H., Nuñez, T. A., & Theobald, D. M. (2016). Achieving climate connectivity in a fragmented landscape. *Proceedings of the National Academy of Sciences USA*, *113*(26), 7195–7200. https://doi.org/10.1073/pnas.1602817113

Monnin, E., Steig, E. J., Siegenthaler, U., Kawamura, K., Schwander, J., Stauffer, B., Stocker, T. F., Morse, D. L., Barnola, J.-M., Bellier, B., Raynaud, D., & Fischer, H. (2004). Evidence for substantial accumulation rate variability in Antarctica during the Holocene, through synchronization of CO2 in the Taylor Dome, Dome C and DML ice cores. *Earth and Planetary Science Letters*, *224*(1–2), 45–54. https://doi.org/10.1016/j.epsl.2004.05.007

Newbold, T. (2010). Applications and limitations of museum data for conservation and ecology, with particular attention to species distribution models. *Progress in Physical Geography*, *34*(1), 3–22. https://doi.org/10.1177/0309133309355630

Ngene, S., Okello, M. M., Mukeka, J., Muya, S., Njumbi, S., & Isiche, J. (2017). Home range sizes and space use of African elephants (*Loxodonta africana*) in the Southern Kenya and Northern Tanzania borderland landscape. *International Journal of Biodiversity and Conservation*, *9*(1), 9–26. https://doi.org/10.5897/IJBC2016.1033

Nogués-Bravo, D., Ohlemüller, R., Batra, P., & Araújo, M. B. (2010). Climate predictors of late Quaternary extinctions. *Evolution: International Journal of Organic Evolution*, *64*(8), 2442–2449. https://doi.org/10.1111/j.1558-5646.2010.01009.x

Ordonez, A., & Williams, J. W. (2013). Climatic and biotic velocities for woody taxa distributions over the last 16 000 years in eastern North America. *Ecology Letters*, *16*(6), 773–781.

Otto-Bliesner, B. L., Brady, E. C., Clauzet, G., Tomas, R., Levis, S., & Kothavala, Z. (2006). Last glacial maximum and Holocene climate in CCSM3. *Journal of Climate*, *19*(11), 2526–2544. https://doi.org/10.1175/JCLI3748.1

Pachzelt, A., Forrest, M., Rammig, A., Higgins, S. I., & Hickler, T. (2015). Potential impact of large ungulate grazers on African vegetation, carbon storage and fire regimes. *Global Ecology and Biogeography*, *24*(9), 991–1002. https://doi.org/10.1111/geb.12313

Pachzelt, A., Rammig, A., Higgins, S., & Hickler, T. (2013). Coupling a physiological grazer population model with a generalized model for vegetation dynamics. *Ecological Modelling*, *263*, 92–102. https://doi.org/10.1016/j.ecolmodel.2013.04.025

Pecl, G. T., Araújo, M. B., Bell, J. D., Blanchard, J., Bonebrake, T. C., Chen, I.-C., Clark, T. D., Colwell, R. K., Danielsen, F., Evengård, B., Falconi, L., Ferrier, S., Frusher, S., Garcia, R. A., Griffis, R. B., Hobday, A. J., Janion-Scheepers, C., Jarzyna, M. A., Jennings, S., … Williams, S. E. (2017). Biodiversity redistribution under climate change: Impacts on ecosystems and human well-being. *Science*, *355*(6332), eaai9214. https://doi.org/10.1126/science.aai9214

Pedersen, M. W., Ruter, A., Schweger, C., Friebe, H., Staff, R. A., Kjeldsen, K. K., Mendoza, M. L., Beaudoin, A. B., Zutter, C., Larsen, N. K., & Potter, B. A. (2016). Postglacial viability and colonization in North America's ice-free corridor. *Nature*, *537*(7618), 45–49.

Peltier, W., Argus, D., & Drummond, R. (2015). Space geodesy constrains ice age terminal deglaciation: The global ICE-6G_C (VM5a) model. *Journal of Geophysical Research: Solid Earth*, *120*(1), 450–487. https://doi.org/10.1002/2014JB011176

Phillips, S. J., & Dudík, M. (2008). Modeling of species distributions with Maxent: New extensions and a comprehensive evaluation. *Ecography*, *31*(2), 161–175. https://doi.org/10.1111/j.0906-7590.2008.5203.x

Phillips, S. J., Dudík, M., & Schapire, R. E. (2020). *Maxent software for modeling species niches and distributions* (version 3.4.1). Retrieved from http://biodiversityinformatics.amnh.org/open_source/maxent/

R Core Team (2020). *R: A language and environment for statistical computing*, Vienna, Austria: R Foundation for Statistical Computing. https://www.R-project.org/

Rabanus-Wallace, M. T., Wooller, M. J., Zazula, G. D., Shute, E., Jahren, A. H., Kosintsev, P., Burns, J. A., Breen, J., Llamas, B., & Cooper, A. (2017). Megafaunal isotopes reveal role of increased moisture on rangeland during late Pleistocene extinctions. *Nature Ecology and Evolution*, *1*(5), 1–5. https://doi.org/10.1038/s41559-017-0125

Radosavljevic, A., & Anderson, R. P. (2014). Making better Maxent models of species distributions: Complexity, overfitting and evaluation. *Journal of Biogeography*, *41*(4), 629–643.

Raia, P., Passaro, F., Fulgione, D., & Carotenuto, F. (2012). Habitat tracking, stasis and survival in Neogene large mammals. *Biology Letters*, *8*(1), 64–66. https://doi.org/10.1098/rsbl.2011.0613

Reimer, P. J., Austin, W. E., Bard, E., Bayliss, A., Blackwell, P. G., Ramsey, C. B., Butzin, M., Cheng, H., Edwards, R. L., Friedrich, M., & Grootes, P. M. (2020). The IntCal20 Northern Hemisphere radiocarbon age calibration curve (0–55 cal kBP). *Radiocarbon*, *62*(4), 725–757.

Ripple, W. J., Wolf, C., Newsome, T. M., Hoffmann, M., Wirsing, A. J., & McCauley, D. J. (2017). Extinction risk is most acute for the world's largest and smallest vertebrates. *Proceedings of the National Academy of Sciences USA*, *114*(40), 10678–10683. https://doi.org/10.1073/pnas.1702078114

Ritchie, J. C., & MacDonald, G. M. (1986). The patterns of post-glacial spread of white spruce. *Journal of Biogeography*, 527–540. https://doi.org/10.2307/2844816

Rivals, F., Mihlbachler, M. C., Solounias, N., Mol, D., Semprebon, G. M., de Vos, J., & Kalthoff, D. C. (2010). Palaeoecology of the Mammoth Steppe fauna from the late Pleistocene of the North Sea and Alaska: Separating species preferences from geographic influence in paleoecological dental wear analysis. *Palaeogeography, Palaeoclimatology, Palaeoecology*, *286*(1–2), 42–54. https://doi.org/10.1016/j.palaeo.2009.12.002

Rule, S., Brook, B. W., Haberle, S. G., Turney, C. S., Kershaw, A. P., & Johnson, C. N. (2012). The aftermath of megafaunal extinction: Ecosystem transformation in Pleistocene Australia. *Science*, *335*(6075), 1483–1486.

Saunders, J. J., Grimm, E. C., Widga, C. C., Campbell, G. D., Curry, B. B., Grimley, D. A., Hanson, P. R., McCullum, J. P., Oliver, J. S., & Treworgy, J. D. (2010). Paradigms and proboscideans in the southern Great Lakes region, USA. *Quaternary International*, *217*(1–2), 175–187. https://doi.org/10.1016/j.quaint.2009.07.031

Schwartz-Narbonne, R., Longstaffe, F. J., Kardynal, K. J., Druckenmiller, P., Hobson, K. A., Jass, C. N., Metcalfe, J. Z., & Zazula, G. (2019). Reframing the mammoth steppe: Insights from analysis of isotopic niches. *Quaternary Science Reviews*, *215*, 1–21. https://doi.org/10.1016/j.quascirev.2019.04.025

Smith, B., Prentice, I. C., & Sykes, M. T. (2001). Representation of vegetation dynamics in the modelling of terrestrial ecosystems: Comparing two contrasting approaches within European climate space. *Global Ecology and Biogeography*, *10*(6), 621–637. https://doi.org/10.1046/j.1466-822X.2001.00256.x

Smith, B., Warlind, D., Arneth, A., Hickler, T., Leadley, P., Siltberg, J., & Zaehle, S. (2014). Implications of incorporating N cycling and N limitations on primary production in an individual-based dynamic vegetation model. *Biogeosciences*, *11*, 2027–2054. https://doi.org/10.5194/bg-11-2027-2014

Smith, F. A., Smith, R. E. E., Lyons, S. K., & Payne, J. L. (2018). Body size downgrading of mammals over the late Quaternary. *Science*, *360*(6386), 310–313.

Strong, W. L., & Hills, L. (2005). Late-glacial and Holocene palaeovegetation zonal reconstruction for central and north-central North America. *Journal of Biogeography*, *32*(6), 1043–1062. https://doi.org/10.1111/j.1365-2699.2004.01223.x

Sukumar, R. (1993). Minimum viable populations for elephant conservation. *Gajah*, *11*, 48–52.

Surovell, T. A., Pelton, S. R., Anderson-Sprecher, R., & Myers, A. D. (2016). Test of Martin's overkill hypothesis using radiocarbon dates on extinct megafauna. *Proceedings of the National Academy of Sciences USA*, *113*(4), 886–891. https://doi.org/10.1073/pnas.1504020112

Surovell, T., Waguespack, N., & Brantingham, P. J. (2005). Global archaeological evidence for proboscidean overkill. *Proceedings of the National Academy of Sciences USA*, *102*(17), 6231–6236. https://doi.org/10.1073/pnas.0501947102

Wang, Y., Porter, W., Mathewson, P. D., Miller, P. A., Graham, R. W., & Williams, J. W. (2018). Mechanistic modeling of environmental drivers of woolly mammoth carrying capacity declines on St. Paul Island. *Ecology*, *99*(12), 2721–2730. https://doi.org/10.1002/ecy.2524

Wang, Y., Shipley, B. R., Lauer, D. A., Pineau, R., & McGuire, J. L. (2020). Plant biomes demonstrate that landscape resilience today is the lowest it has been since end-Pleistocene megafaunal extinctions. *Global Change Biology*, *26*(10), 5914–5927. https://doi.org/10.1111/gcb.15299

Waters, M. R. (2019). Late Pleistocene exploration and settlement of the Americas by modern humans. *Science*, *365*(6449), eaat5447.

Widga, C., Hodgins, G., Kolis, K., Lengyel, S., Saunders, J., Walker, J. D., & Wanamaker, A. D. (2020). Life histories and niche dynamics in late Quaternary proboscideans from midwestern North America. *Quaternary Research*, 1–16. https://doi.org/10.1017/qua.2020.85

Widga, C., Lengyel, S. N., Saunders, J., Hodgins, G., Walker, J. D., & Wanamaker, A. D. (2017). Late Pleistocene proboscidean population dynamics in the North American Midcontinent. *Boreas*, *46*(4), 772–782.

Willerslev, E., Davison, J., Moora, M., Zobel, M., Coissac, E., Edwards, M. E., Lorenzen, E. D., Vestergård, M., Gussarova, G., Haile, J., Craine, J., Gielly, L., Boessenkool, S., Epp, L. S., Pearman, P. B., Cheddadi, R., Murray, D., Bråthen, K. A., Yoccoz, N., … Taberlet, P. (2014). Fifty thousand years of Arctic vegetation and megafaunal diet. *Nature*, *506*(7486), 47–51. https://doi.org/10.1038/nature12921

Williams, J. W., Burke, K. D., Crossley, M. S., Grant, D. A., & Radeloff, V. C. (2019). Land-use and climatic causes of environmental novelty in Wisconsin since 1890. *Ecological Applications*, *29*(7), e01955. https://doi.org/10.1002/eap.1955

Williams, J. W., Grimm, E. C., Blois, J. L., Charles, D. F., Davis, E. B., Goring, S. J., Graham, R. W., Smith, A. J., Anderson, M., Arroyo-Cabrales, J., Ashworth, A. C., Betancourt, J. L., Bills, B. W., Booth, R. K., Buckland, P. I., Curry, B. B., Giesecke, T., Jackson, S. T., Latorre, C., … Takahara, H. (2018). The Neotoma Paleoecology Database, a multiproxy, international, community-curated data resource. *Quaternary Research*, *89*(01), 156–177. https://doi.org/10.1017/qua.2017.105

Williams, J. W., Shuman, B. N., Webb, T., Bartlein, P. J., & Leduc, P. L. (2004). Late-Quaternary vegetation dynamics in North America: Scaling from taxa to biomes. *Ecological Monographs*, *74*(2), 309–334. https://doi.org/10.1890/02-4045

Williams, J. W., Tarasov, P., Brewer, S., & Notaro, M. (2011). Late Quaternary variations in tree cover at the northern forest-tundra ecotone. *Journal of Geophysical Research: Biogeosciences*, *116*. G01017.

Wroe, S., Field, J. H., Archer, M., Grayson, D. K., Price, G. J., Louys, J., Faith, J. T., Webb, G. E., Davidson, I., & Mooney, S. D. (2013). Climate change frames debate over the extinction of megafauna in Sahul (Pleistocene Australia-New Guinea). *Proceedings of the National Academy of Sciences USA*, *110*(22), 8777–8781. https://doi.org/10.1073/pnas.1302698110

Zimov, S., Zimov, N., Tikhonov, A., & Chapin, F. III (2012). Mammoth steppe: A high-productivity phenomenon. *Quaternary Science Reviews*, *57*, 26–45. https://doi.org/10.1016/j.quascirev.2012.10.005

Zuo, W., Smith, F. A., & Charnov, E. L. (2013). A life-history approach to the late Pleistocene megafaunal extinction. *The American Naturalist*, *182*(4), 524–531. https://doi.org/10.1086/671995

BIOSKETCH

Yue Wang is a postdoctoral researcher at Georgia Institute of Technology. Her research interests include how organisms adapt (or fail to adapt) to climate change using both biodiversity databases and model simulations from site-level to continental scales. An important component of her research work is to examine terrestrial plant resilience and how it culminates in animal extinctions given climate change and human activity.

SUPPORTING INFORMATION

Additional supporting information may be found online in the Supporting Information section.

How to cite this article: Wang Y, Widga C, Graham RW, et al. Caught in a bottleneck: Habitat loss for woolly mammoths in central North America and the ice-free corridor during the last deglaciation. *Global Ecol Biogeogr.* 2020;00:1–16. https://doi.org/10.1111/geb.13238